

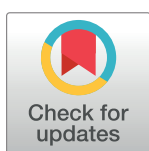
## RESEARCH ARTICLE

# Characterisation and genome sequence of the lytic *Acinetobacter baumannii* bacteriophage vB\_AbaS\_Loki

Dann Turner<sup>1</sup>, Matthew E. Wand<sup>2</sup>, Yves Briers<sup>3,4</sup>, Rob Lavigne<sup>4</sup>, J. Mark Sutton<sup>2</sup>, Darren M. Reynolds<sup>1\*</sup>

**1** Centre for Research in Biosciences, Department of Applied Sciences, Faculty of Health and Applied Sciences, University of the West of England, Coldharbour Lane, Bristol, United Kingdom, **2** National Infections Service, Public Health England, Porton Down, Salisbury, Wiltshire, United Kingdom, **3** Laboratory of Applied Biotechnology, Department of Applied Biosciences, Ghent University, Ghent, Belgium, **4** Laboratory of Gene Technology, Biosystems Department, KU Leuven, Heverlee, Belgium

\* [darren.reynolds@uwe.ac.uk](mailto:darren.reynolds@uwe.ac.uk)



## OPEN ACCESS

**Citation:** Turner D, Wand ME, Briers Y, Lavigne R, Sutton JM, Reynolds DM (2017) Characterisation and genome sequence of the lytic *Acinetobacter baumannii* bacteriophage vB\_AbaS\_Loki. PLoS ONE 12(2): e0172303. doi:10.1371/journal.pone.0172303

**Editor:** Mark J. van Raaij, Centro Nacional de Biotecnología, SPAIN

**Received:** November 15, 2016

**Accepted:** February 2, 2017

**Published:** February 16, 2017

**Copyright:** © 2017 Turner et al. This is an open access article distributed under the terms of the [Creative Commons Attribution License](https://creativecommons.org/licenses/by/4.0/), which permits unrestricted use, distribution, and reproduction in any medium, provided the original author and source are credited.

**Data Availability Statement:** All relevant data are within the paper and its Supporting Information files.

**Funding:** This work was supported by a QR2015 award from the University of the West of England, Bristol to D.T. R.L. is supported by a the Geconcerteerde Onderzoeks Actie grant 'Phage Biosystems' from KU Leuven. R.L. & Y.B. are members of the FWO research community 'Phagebiotics'. The funders had no role in study

## Abstract

*Acinetobacter baumannii* has emerged as an important nosocomial pathogen in healthcare and community settings. While over 100 of *Acinetobacter* phages have been described in the literature, relatively few have been sequenced. This work describes the characterisation and genome annotation of a new lytic *Acinetobacter* siphovirus, vB\_AbaS\_Loki, isolated from activated sewage sludge. Sequencing revealed that Loki encapsulates a 41,308 bp genome, encoding 51 predicted open reading frames. Loki is most closely related to *Acinetobacter* phage IME\_AB3 and more distantly related to *Burkholderia* phage KL1, *Paracoccus* phage vB\_PmaS\_IMEP1 and *Pseudomonas* phages vB\_Pae\_Kakheti25, vB\_PaeS\_SCH\_Ab26 and PA73. Loki is characterised by a narrow host range, among the 40 *Acinetobacter* isolates tested, productive infection was only observed for the propagating host, *A. baumannii* ATCC 17978. Plaque formation was found to be dependent upon the presence of Ca<sup>2+</sup> ions and adsorption to host cells was abolished upon incubation with a mutant of ATCC 17978 encoding a premature stop codon in *lpxA*. The complete genome sequence of vB\_AbaS\_Loki was deposited in the European Nucleotide Archive (ENA) under the accession number LN890663.

## 1 Introduction

Since 1966 more than 100 bacteriophages specific for the genus *Acinetobacter* have been reported in the literature, belonging to the families *Leviviridae*, *Myoviridae*, *Podoviridae* and *Siphoviridae* [1]. A total of 39 complete genome sequences are presently available for bacteriophages infecting *Acinetobacter* spp., representing less than 1% of all publicly available phage genome sequences. Two groups of *Acinetobacter* phages have recently been recognised as new genera by the International Committee for the Taxonomy of Viruses, the *Ap22virus* and *Fri1-virus* belonging to the families *Myoviridae* and *Podoviridae*, respectively. While 19 siphoviruses infecting *A. baumannii* have been described, only four have been sequenced; YMC11/11/R3177 [2], Bphi-B1251 [3], IME\_AB3 and the induced prophage vB\_AbaS\_TRS1 [4].

design, data collection and analysis, decision to publish, or preparation of the manuscript.

**Competing interests:** The authors have declared that no competing interests exist.

Interest in bacteriophages infecting species of *Acinetobacter* has increased in recent years, primarily due to the emergence of *A. baumannii* as a prominent multiple-drug resistant nosocomial pathogen, responsible for significant outbreaks of disease both in the UK and worldwide [5]. Due to a capacity to persist for extended periods in a dry environment [6] and resistance to treatment with disinfectants [7], combined with intrinsic and acquired antibiotic resistance [8], the control and therapeutic management of *A. baumannii* has become a pressing concern. A wide array of resistance mechanisms have been described for *A. baumannii* and strains with resistance to multiple antibiotics have been reported worldwide [9]. Colistin (polymixin B) has often been cited as the antibiotic of last resort for treatment of *Acinetobacter*, particularly in respiratory infections, but resistant strains have been widely reported in clinical settings [10]. Recent research suggests that *A. baumannii* appears to be able to readily adapt to colistin exposure [11], raising the probability of pan-drug resistance arising in this species in the near future.

The characterisation of bacteriophages facilitates a greater understanding of their biology, including host specificity, genomic diversity and adaptation to their bacterial hosts, facilitating their subsequent exploitation as therapeutic agents or as a resource for the development of genetic tools. In the present study, we report the isolation, characterisation and complete genome sequence of bacteriophage Loki (vB\_AbaS\_Loki), a new member of the *Siphoviridae* infecting *A. baumannii*.

## 2 Results

### 2.1 Virion morphology

Loki was isolated from activated sludge following enrichment with *A. baumannii* ATCC 17978. Examination by transmission electron microscopy (Fig 1) revealed Loki to be a B1 siphovirus that resembles *Burkholderia* phage vB\_BceS\_KL1 [12]. Loki and KL1 share a similar morphology to the flagellum-specific Enterobacteria phage chi ( $\chi$ ) but lack the characteristic single long terminal tail fibre of this phage (H.-W. Ackermann, personal communication). The capsid is isometric, measuring  $57 \pm 4$  nm across opposite apices. The non-contractile tail exhibits transverse striations, measures  $176 \pm 3$  nm in length and  $10 \pm 0.9$  nm in diameter with short tail spikes present at the tail terminus.

### 2.2 Adsorption and one-step growth

Under conditions of one-step growth, the latent period was determined as 40 minutes with a rise period lasting a further 30 minutes yielding a burst size of 43 p.f.u per infective centre. An average burst size of  $40 \pm 5.8$  p.f.u. per infective centre was determined for single burst experiments. The eclipse period was not determined. Loki exhibited an adsorption rate constant of  $1.32 \times 10^{-8}$  ml/min to cells of *A. baumannii* ATCC 17978 at 30°C (Fig 2). Adsorption was abolished using a mutant of ATCC 17978 that had undergone a single point mutation in *lpxA* (E216Stop) following exposure to sub-MIC concentrations of colistin [11]. The introduction of a premature termination codon results in the truncation of LpxA from 262 to 216 amino acids. LpxA is a critical enzyme in the biosynthesis of lipid A and mutations to this gene have been demonstrated to result in the complete loss of lipopolysaccharide (LPS) biosynthesis in *A. baumannii* ATCC 19606 and a concomitant increase in resistance to colistin [13]. This evidence suggests that the host cell surface receptor utilised by Loki might be a component of LPS. ATCC 17978 possess a smooth form of LPS in addition to an exopolysaccharide capsule [14]. Phages of Gram-negative bacteria use a variety of cell surface structures that include flagella, pili, outer membrane proteins as well as the O-antigen, inner and outer core polysaccharides of LPS for host recognition [15,16].

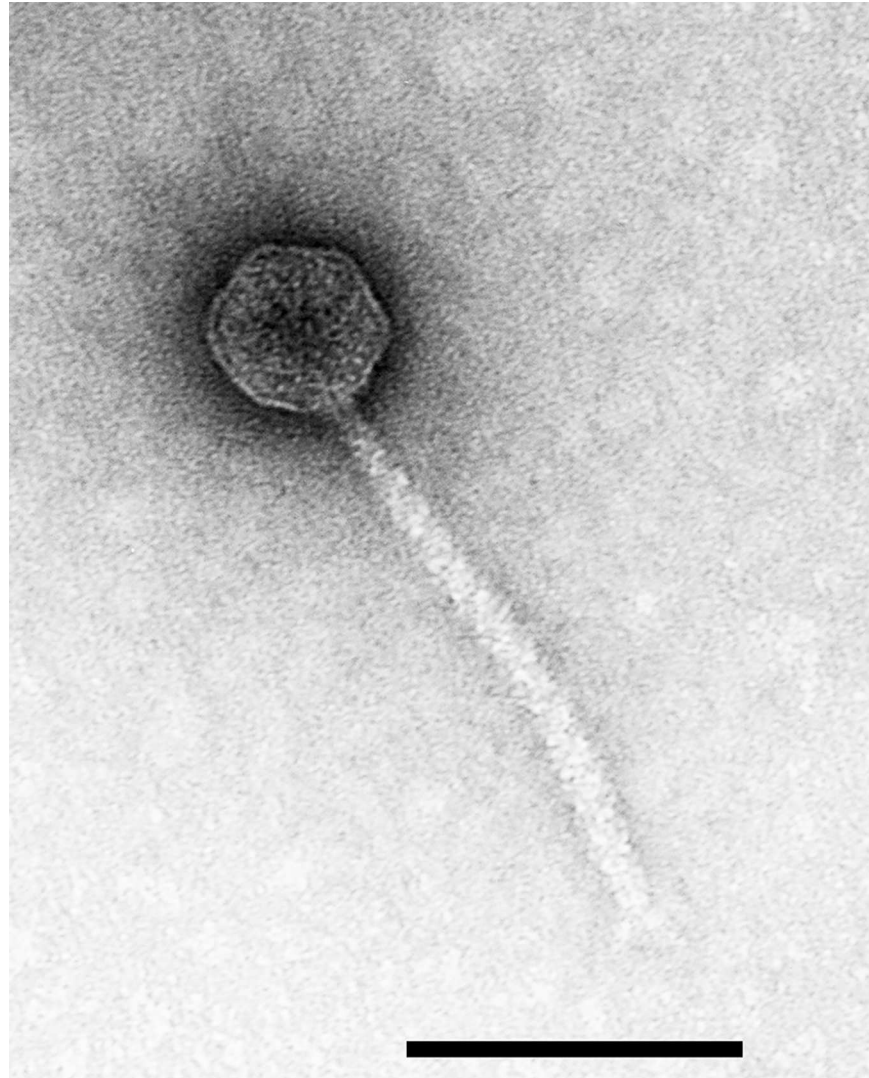


**Fig 1. Transmission electron micrograph of Loki negatively stained with 2% w/v uranyl acetate.** The scale bar represents 100 nm.

doi:10.1371/journal.pone.0172303.g001

### 2.3 Host range and efficiency of plating (EOP)

Loki forms small, turbid plaques on *A. baumannii* ATCC 17978 of average size  $0.5 \pm 0.1$  mm after incubation at  $30^{\circ}\text{C}$ . Plaques ceased to expand after 16 hours of incubation. Titres determined using overlay agar plaque assays were unaffected after treatment of phages with chloroform. The requirement for calcium ions to expedite plaque formation was investigated by varying the concentration of calcium chloride added to overlay and underlay agar. The ability of Loki to form plaques was strictly dependent upon the presence of  $\text{Ca}^{2+}$ , whereas titres were unaffected by the presence or absence of  $\text{Mg}^{2+}$  at  $10 \text{ mmol l}^{-1}$ . Overlay plates prepared without  $5 \text{ mmol l}^{-1} \text{CaCl}_2$  yielded no plaques and omission of  $\text{CaCl}_2$  from the bottom agar reduced the number of plaques by approximately 50% (Table 1).

A number of *Siphoviridae* infecting both Gram-positive and Gram-negative hosts have been demonstrated to depend upon the presence of  $\text{Ca}^{2+}$  ions, including *Mycobacterium* phage L5 [17], *Escherichia* phage T5 [18], *Bacillus* phage SF6 [19] and the 936 group of *Lactococcus*

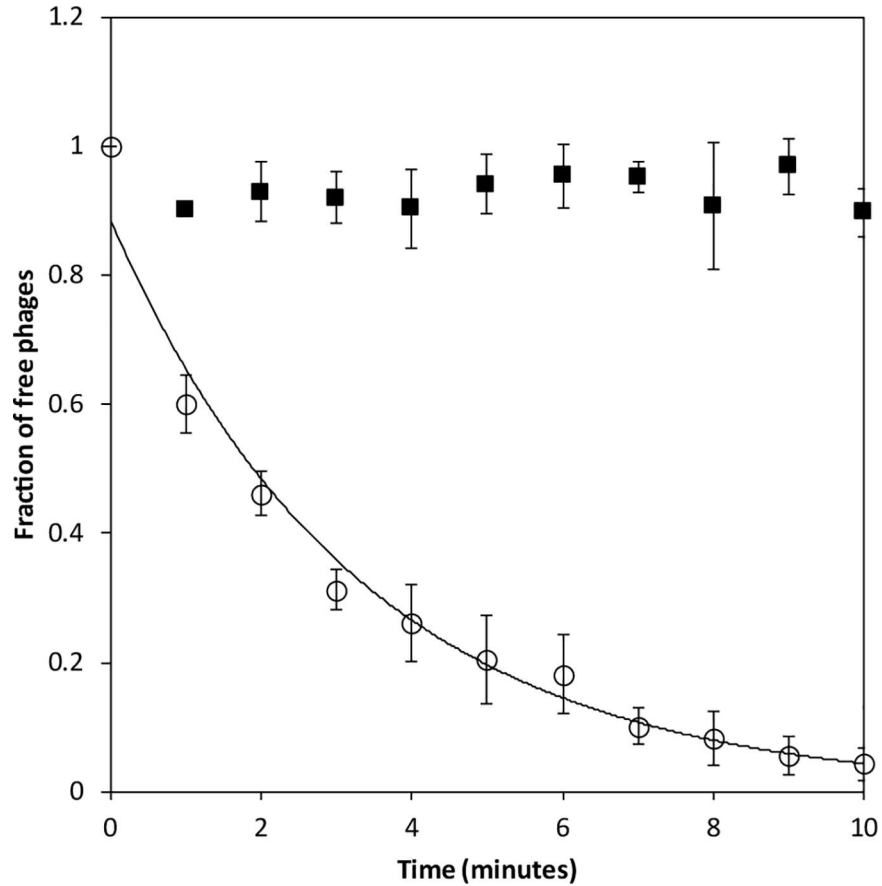


**Fig 2. Adsorption of Loki to *A. baumannii* ATCC 17978 (open circles) and IpxA mutant (filled squares).** The fraction of free phages remaining in solution is plotted over time. Error bars denote standard deviation (n = 5).

doi:10.1371/journal.pone.0172303.g002

phages [20]. The requirement for  $\text{Ca}^{2+}$  has been shown to affect either adsorption, transfer of the phage genome or the formation of progeny virions in these phages. Notably, while zones of clearing were evident on spot plates of the propagating host, individual plaques were not observed on overlay plaque assays at an incubation temperature of 37°C. A similar lysis phenotype was previously observed by Lynch et al., during their characterisation of the related *Burkholderia cepacia* phage KL1 [12].

Loki exhibited broad tropism under spot plate conditions at 30°C, forming zones of clearing against type strains and clinical isolates of *A. baumannii* encompassing all three international clonal lineages (S1 Table). Zones of clearing were observed for 36 of 38 strains (95%) of *A. baumannii* in addition to a single strain of *A. lwoffii* and *A. baylyi*. This broad host range was not reflected in subsequent titrations to determine EOP where plaque formation was not

**Table 1.  $\text{Ca}^{2+}$ -dependent infection of *A. baumannii* ATCC 17978.** Titres are the mean of triplicate assays. Values in parenthesis are the efficiencies of plating compared with the titre on *A. baumannii* ATCC 17978 in the presence of 5 mmol l<sup>-1</sup>  $\text{Ca}^{2+}$ .

p.f.u ml <sup>-1</sup> <i>A. baumannii</i> ATCC 17978		
+5 mmol l <sup>-1</sup> $\text{Ca}^{2+}$ (overlay and underlay agar)	+5 mmol l <sup>-1</sup> $\text{Ca}^{2+}$ (overlay agar alone)	0 mmol l <sup>-1</sup> $\text{Ca}^{2+}$
7.43 x 10 <sup>8</sup> (1)	3.64 x 10 <sup>8</sup> (0.49)	No plaques (0)

doi:10.1371/journal.pone.0172303.t001

observed at any dilution for any of the *Acinetobacter* strains tested other than the propagating host. The discrepancy between these results confirms the necessity of EOP when assessing the host range of a new phage isolate. Efficiency of plating represents a more stringent assessment of host range, since with low number of phages plaques can only be formed by productive infection, that is, through the production and release of viable progeny virions through cell lysis. The zones of clearing observed under spot plate conditions may have arisen as the result of adsorption of large numbers of phage causing destabilisation of the outer membrane; the classical definition of lysis from without [21]. Alternatively, these zones of clearing may have arisen from the presence of bacteriocins in the phage preparation [22] or potentially, abortive infection resulting in the inhibition of phage replicative processes [23]. Loki did not cause lysis against either *Escherichia coli* K12, *Pseudomonas fluorescens* NCIMB 9046, *Burkholderia cepacia* NCIMB 9088 or *Klebsiella pneumoniae* NCTC 10896.

## 2.4 Genome sequence

Sequencing of phage Loki yielded a single contig with a high average coverage of 3,435x. Loki has a linear dsDNA genome of 41,308 bp with a G+C content of 44.35%, slightly higher than that exhibited by most *A. baumannii* genomes, for which the GC contents of available genome sequences range between 38.7% and 42.6%.

Undigested Loki genomic DNA yielded a single high molecular weight band estimated at 42,100 bp when resolved by PFGE, approximately 800 bp greater than the sequenced genome assembly. The sequence assembly was circular, indicating that the Loki genome is either circularly permuted or has a non-permuted terminal redundancy, e.g. direct terminal repeats. Several types of termini among the *Caudovirales* have been studied including, but not limited to, single stranded 3' and 5' cohesive ends, short and long non-permuted direct terminal repeats, covalently bound terminal proteins, terminal host sequences and circularly permuted direct terminal repeats [24,25].

Banding patterns after digestion of Loki genomic DNA with restriction enzymes were in agreement with those predicted *in silico* from the genome sequence, assuming a circular conformation (Figure A in [S1 File](#)). In order to discount the presence of cohesive ends at the genome termini, Loki genomic DNA digested with either BmtI, BsrGI or BclI was denatured by heating at 80°C followed by rapid or slow cooling (Figure B in [S1 File](#)). If the genome has cohesive ends, the two restriction fragments possessing the cohesive termini will anneal in the slow cooled sample and form a single larger fragment [24]. No alteration to the restriction profile was observed between the rapid and slow cooled samples. Additionally, treatment of Loki genomic DNA with T4 DNA ligase prior to digestion did not alter the pattern of restriction fragments (Figure C in [S1 File](#)). If cohesive termini were present, ligation would cause the two restriction fragments containing the termini to appear as a single fragment the sum of the respective sizes. Cohesive ends can therefore be excluded. Time limited digestion with the exonuclease BAL-31 followed by digestion with BmtI, BsrGI, BclI or SspI resulted in an even, simultaneous degradation of all restriction fragments (Figures D-G in [S1 File](#)). These results discount the presence of fixed termini, such as direct terminal repeats, where a progressive shortening of two restriction fragments containing the fixed termini due to exonuclease activity would have been observed [26]. The simultaneous degradation of all restriction fragments indicates that the position Loki genomic termini are variable, representing a population comprised of many different end positions. Circularly permuted genomes are characteristic of a head-full packaging strategy, where the packaged DNA length is between 102 and 110% of the total genome length, resulting in terminal redundancy [24]. No submolar packaging (*pac*) fragment associated with the terminase initiation cleavage site was observed on electrophoresis



gels. Taken together, these data suggest that the Loki genome is circularly permuted and terminally redundant. Head-full packaging has been associated with generalised transduction, a characteristic that has the potential to facilitate horizontal transfer of host DNA [24].

The genome sequence is opened at the small terminase subunit, according to convention [24]. A total of 51 open reading frames (ORFs) were predicted, representing a coding percentage of 95.4% at a density of 1.23 genes per kb. No tRNAs or rRNAs were identified and putative functions could be assigned for 31 (60%) of the ORFs after analysis using BLASTP, HHblits, HHsearch, Pfam and InterProScan (S2 File). No putative gene products with similarities to proteins involved in lysogeny or host conversion were found, which appears to confirm that Loki is a strictly lytic phage.

As has been observed for many *Siphoviridae* [27,28], the Loki genome is organised into discrete functional modules (Fig 3) containing genes involved in virion morphogenesis (gp01-gp21), DNA replication (gp22-gp33) and a final module encoding early genes and those involved in cell lysis (gp34-gp51).

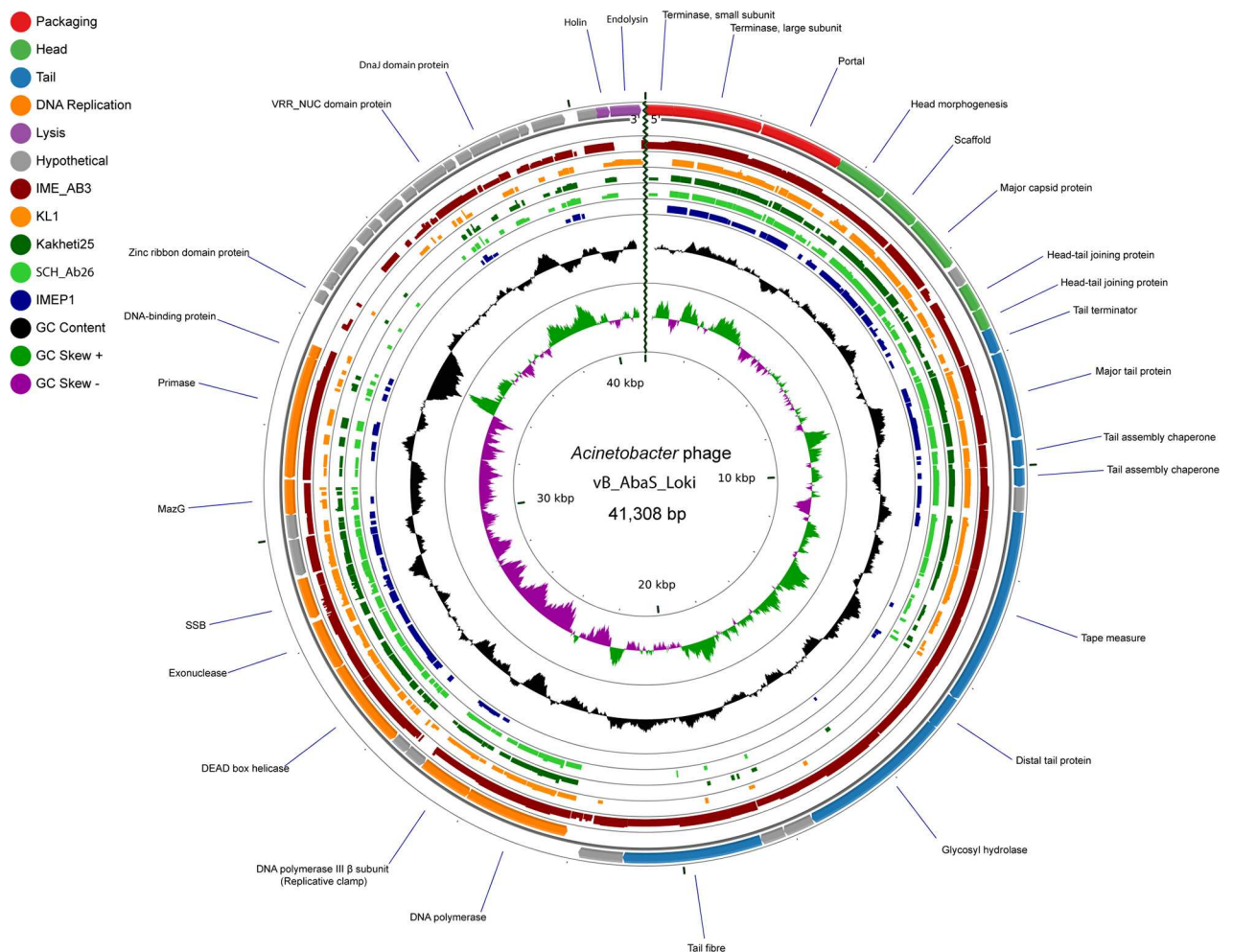


**Fig 3. Comparative genome map of Loki prepared using the CGView Comparison Tool [29].** The outer ring illustrates ORFs encoded by Loki, coloured according to putative function as shown in the key. TBLASTX was used to compare sequence similarity with the related phages IME\_AB3 [KF811200], KL1 [JF939047], vB\_Pae\_Kakheti25 [JQ307387], SCH\_Ab26 [HG962376] and IMEP1 [KP162168], shown in red, orange, green, light green and blue, respectively. GC content is depicted in black, while positive and negative GC skew is shown as green and purple, respectively.

doi:10.1371/journal.pone.0172303.g003

**2.4.1 Packaging, morphogenesis and structural proteins.** Genes encoding assembly chaperones and the mature virion structural protein components are located in a continuous module comprising 21 ORFs, representing 39.2% of the total encoded genes. The genes in this module follows the classical *Siphoviridae* organisation; genes encoding the DNA packaging apparatus are followed by those encoding the head, head-tail joining, the tail and adsorption apparatus [27]. Analysis of CsCl-purified virions using 1D SDS-PAGE resolved 11 protein bands, representing virion structural components, with molecular weights ranging from 12 to 108 kDa (Fig 4). The two predominant bands at 54 and 35 kDa are suggestive of major capsid and major tail proteins, respectively and correspond to the predicted molecular weight of these proteins.

Based upon searches conducted using BLASTP and HHsuite (S2 File) the functions of 16 gene products (76%) involved in virion structure and morphogenesis could be identified. The DNA packaging apparatus of tailed phages consists of a heterodimeric terminase composed of small and large subunits where the small subunit is responsible for DNA binding and the large terminase mediates prohead binding and cleavage of concatameric phage DNA into individual genome units. The Loki small terminase subunit was assigned on the basis of synteny and homologs identified using PSI-BLAST. The large terminase contains a Pfam Terminase\_6 domain (PF03237) and is encoded immediately upstream of the portal vertex protein (DUF4055). Gene products identified to play a role in capsid assembly include a SPP1 gp7 family morphogenesis protein (gp04) (PFAM PF04233), scaffold (gp05) and major capsid protein (gp06). Two proteins were identified to play a putative role in head-tail joining, gp08 and gp09 that showed similarity to the connector proteins gp6 of HK97 (PDB 3jvo) and gpFII (PDB 1k0h) of Lambda, respectively [30,31]. Gp10 shows significant similarity to the tail terminator proteins gp17 (PDB 2lfp) of *Bacillus* phage SPP1 and the minor tail protein gpU (PDB 3fz2) of Lambda. These proteins play an essential role in tail assembly, terminating tail polymerisation and providing a surface for interaction between the mature phage head and tail [32,33].

The major tail protein (gp11) was assigned on the basis of synteny and a weak match to the major tail protein, GpV, of Lambda (PDB 2k4q). In many tailed phages, correct formation of the tail is dependent upon the expression of two chaperones, one of which is produced as a fusion product by appending an additional C-terminal domain via a programmed translational -1 frameshift. Tail chaperones produced through frameshifts have been confirmed experimentally for phages  $\lambda$ , P2, L5, TM4, phiC31, HK022, and HK97 [34–37]. The presence of a frameshift motif AAAAAAC immediately adjacent to the stop codon of gp12 would suggest a similar frameshift event may occur in Loki resulting in a fusion product of gp12 and gp13. An identical motif is found in the tail assembly chaperone of IME\_AB3 (locus\_tag: IME\_AB3\_31).

A further gene product predicted to be involved in tail assembly protein, gp14, is encoded between the tape measure and assembly chaperones for which HHsearch identified a HK97 gp10-like domain (PF04883) with high probability. The putative tape measure, gp15, was identified by the presence of a conserved domain (IPR013491 tape\_meas\_nterm), a predicted coiled coil structure and by homologs in other phages and prophages identified by BLASTP. Gene products encoded by gp16 through gp21 are predicted to encode products that comprise the distal tail tip complex and facilitate adsorption to host cells. PSI-BLAST searches linked gp16 with the distal tail protein pb9 of phage T5 and other T5-like phages EPS7, SPC35 and Akfv33 after three iterations. In addition, HHsearch returned a significant match to pdb9 (PDB: 4jmq). The T5 pdb9 protein has been suggested to represent a large family of distal tail proteins that are found in numerous siphoviruses and which form a hexameric ring that serves to connect the tail tube to the adsorption apparatus [38]. The function of gp17 is not clear but HHsearch returned matches to hydrolases in the pdb70 and pfam27 HHsuite databases. Gene

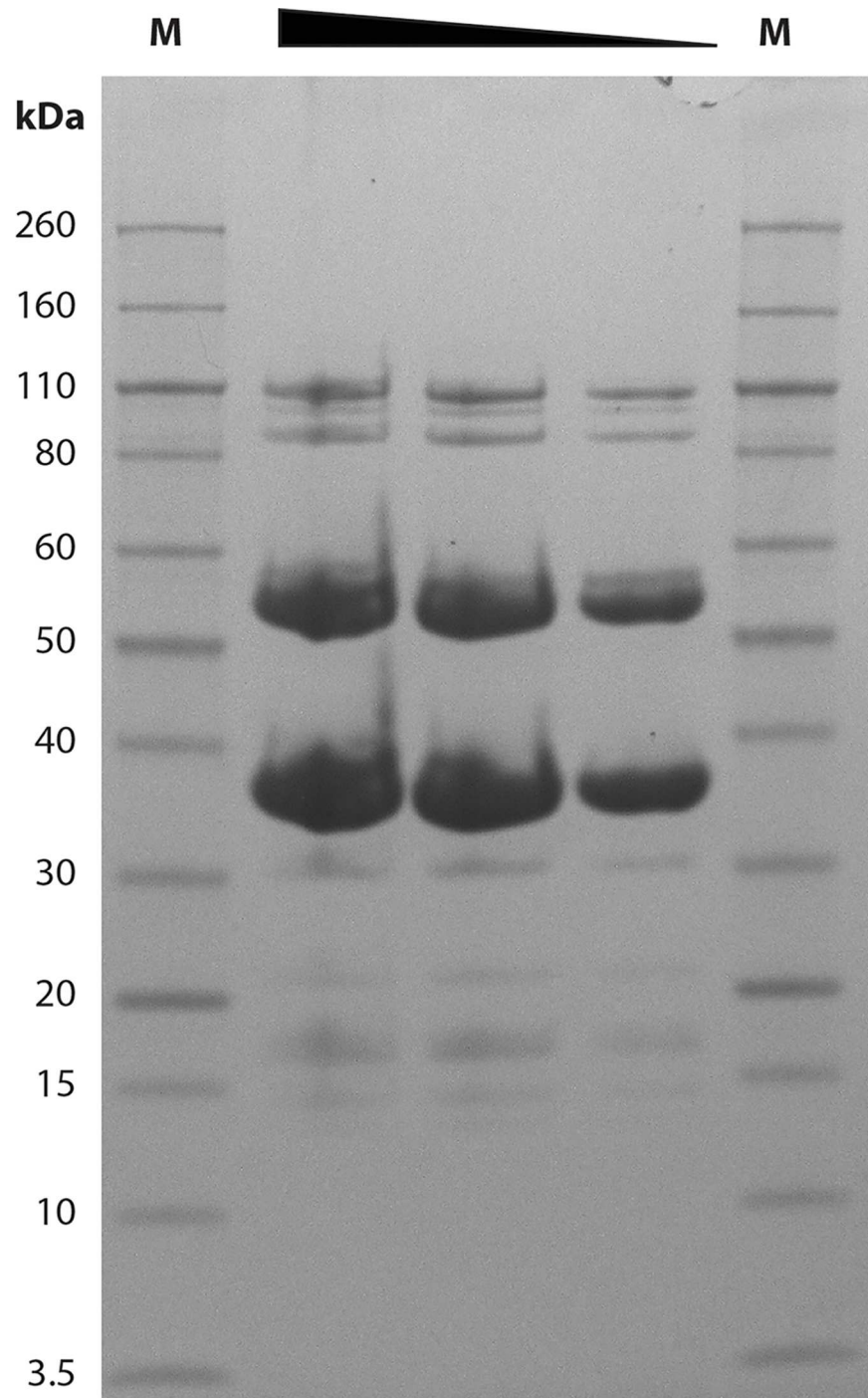


**Fig 4. 1D SDS-PAGE of structural proteins from CsCl-purified Loki virions.** Lanes containing protein standard ladders are labelled M and the sizes of markers in kilodaltons (kDa) are shown on the left. The triangle depicts decreasing concentrations of loaded protein.

doi:10.1371/journal.pone.0172303.g004

product 18 is also likely to form part of the tail tip complex, indicated by a weak match to the gp44 baseplate hub protein of the temperate myovirus Mu (PDB: 1wru) and a significant match to the lambda minor tail protein L domain (PF05100) using HHsearch. For gp19, searches conducted with HHsearch against the Pfam28 and pdb70 databases returned matches



to bacteriophage peptidoglycan hydrolases and bacterial cell wall hydrolases, respectively, that might suggest a role for gp19 in facilitating translocation of the virion DNA across the bacterial cell wall. The putative tail fibre, gp20 was assigned this function due to the presence of a fibronectin-like domain (Pfam: PF13550 Phage-tail\_3) commonly associated with phage tail fibres. No function could be assigned to gp21.

**2.4.2 DNA replication gene module.** Putative functions could be predicted for nine gene products encoded by the replication cluster. Loki encodes a putative family B DNA polymerase (Gp22), DNA polymerase III  $\beta$  subunit (gp23), helicase (gp26), single stranded DNA binding protein (gp28) and primase (gp32). In addition Loki encodes a putative exonuclease (gp27), a DUF3987 domain protein (gp32) and a protein linked to a SprT-like and peptidase domains by HHsearch (gp24). A notable feature is the presence of a MazG domain protein (gp31) within the DNA replication module. In *E. coli* MazG is a nucleotide pyrophosphohydrolyase that is able to hydrolyse all canonical nucleoside triphosphates, has been demonstrated to act as a regulator of the stringent response by interaction with Era and inactivation of ppGpp [39]. Proteins containing the MazG domain have previously been identified in marine phages as well as those infecting diverse bacterial genera that include phages closely related to Loki [12,40–43]. While no functional assays have yet been performed to demonstrate that these phage proteins act as MazG homologs, it has been suggested that these MazG domain proteins might act to extend the logarithmic phase of bacterial growth, facilitating the production of progeny virions through the reactivation of metabolic pathways that are usually suppressed under conditions of nutrient starvation [41].

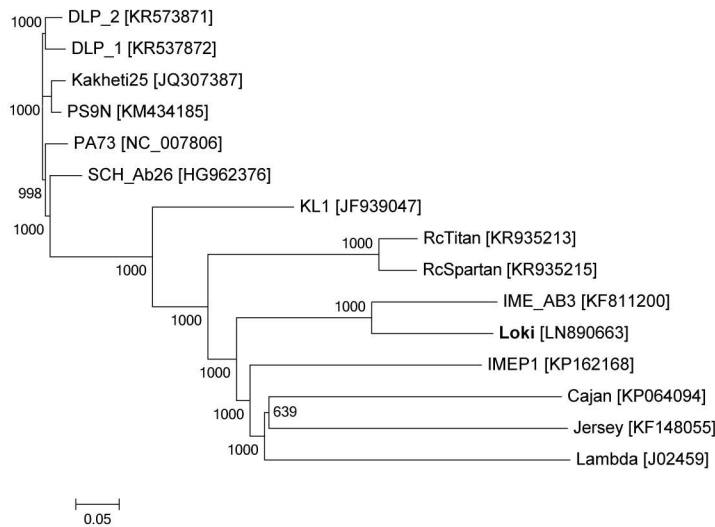
**2.4.3 Early/Lysis gene module.** Putative functions could be assigned for only five from a total of 18 ORFs present in the early/lysis gene module. A zinc ribbon domain (PF13248) protein, gp35, was identified using HHsearch and gp42 encodes a VRR\_NUC domain. An incomplete C-terminal cysteine-rich DnaJ domain (IPR001305) was predicted for gp45 by InterProScan, with two conserved CXXCXGXG motifs while HHsearch identified a significant match to the antitermination protein Q of lambda (PDB: 4mo1).

Genes identified to play a role in host cell lysis consisted of a putative class I holin (gp50) with two predicted transmembrane domains encoded immediately upstream of the putative endolysin (gp51) that contains an N-acetylmuraminidase (pfam: PF09374) and a C-terminal peptidoglycan binding domain (Pfam: PF05838). Modular endolysins are relatively rare in phages infecting Gram-negative hosts, most produce endolysins comprised of a single domain that acts upon a specific peptidoglycan bond. All modular endolysins active against Gram-negative bacteria described to date contain a conserved repeat sequence in the peptidoglycan-binding domain [44]. The Loki endolysin contains a single copy, albeit less conserved, of this motif.

## 2.5 Relationships between Loki and other *Siphoviridae*

Searches conducted using dc-megablast and megablast revealed significant nucleotide similarity between Loki and *Acinetobacter* phage IME\_AB3 and these two phages exhibit significant synteny across the entire genome. Additional relationships with *Burkholderia* phage vB\_BceS\_KL1 [12], *Paracoccus* phage vB\_PmaS\_IMEP1, *Stenotrophomonas* phages DLP1 and DLP2 [43], *Rhodobacter* phages RcTitan and RcSpartan [45], as well as *Pseudomonas* phages vB\_Pae\_Kakheti25 [46], vB\_PaeS\_SCH\_Ab26 and PA73 [47] were also identified using TBLASTX. To perform pairwise comparisons, genomes were co-linearised to start at the small terminase subunit and aligned using ClustalX (Fig 5A) and EMBOSS Stretcher (Fig 5B). At the protein level, CoreGenes3.5 was used to calculate the percentage value of gene products conserved between each phage (Fig 5C).

**A**



**B**

Name	DLP_2	DLP_1	Kakheti25	PS9N	PA73	SCH_Ab26	KL1	RcTitan	RcSpartan	IME_AB3	Loki	IMEP1
DLP_2	100	94.5	94.4	95.2	93.8	91.8	67.3	54.6	54.5	50.7	50.6	52.4
DLP_1	94.5	100	93.5	94.8	93.5	91.5	67.4	54.6	54.5	50.7	50.4	52.5
Kakheti25	94.4	93.5	100	96.4	93.6	92.7	67.6	54.7	54.5	50.7	50.5	52.4
PS9N	95.2	94.7	96.4	100	93.3	92.7	67.4	54.7	54.6	50.7	50.5	52.4
PA73	93.8	93.5	93.6	93.3	100	92.2	67.2	54.6	54.4	50.8	50.5	52.5
SCH_Ab26	91.8	91.5	92.7	92.8	92.2	100	67.1	54.7	54.5	51	50.6	52.4
KL1	67.4	67.5	67.6	67.4	67.2	67.1	100	54.3	54	50.7	50.4	52.2
RcTitan	54.6	54.6	54.7	54.7	54.6	54.6	54.3	100	89.6	49.5	48.4	51.8
RcSpartan	54.4	54.5	54.5	54.6	54.3	54.5	54	89.5	100	49.5	48.8	51.9
IME_AB3	50.7	50.6	50.7	50.7	50.7	51	50.7	49.5	49.5	100	67.9	49.5
Loki	50.6	50.4	50.4	50.5	50.5	50.5	50.4	48.5	48.8	67.9	100	48.8
IMEP1	52.3	52.4	52.3	52.4	52.5	52.4	52.2	51.7	51.9	49.6	48.8	100

**C**

Name	DLP_2	DLP_1	Kakheti25	PS9N	PA73	SCH_Ab26	KL1	RcTitan	RcSpartan	IME_AB3	Loki	IMEP1	Cajan	Jersey	Chi	Lambda
DLP_2	100	96.49	93.1	92.59	94.23	92.31	80	50.82	47.54	54.39	56.86	48.08	13.19	8.7	6.67	3.03
DLP_1	94.83	100	89.66	90.74	92.31	92.31	80	52.46	49.18	54.39	58.82	50	14.29	8.7	5.33	4.55
Kakheti25	91.38	89.47	100	92.59	90.38	96.15	83.64	50.82	47.54	52.63	58.82	46.15	13.19	8.7	5.33	3.03
PS9N	86.21	85.96	86.21	100	88.46	84.62	80	50.82	47.54	50.88	54.9	46.15	14.29	8.7	5.33	4.55
PA73	84.48	80.7	82.76	85.19	100	84.62	76.36	52.46	49.18	54.39	56.86	48.08	14.29	8.7	5.33	3.03
SCH_Ab26	82.76	84.21	87.93	81.48	84.62	100	78.18	50.82	49.18	50.88	54.9	48.08	14.29	8.7	6.67	3.03
KL1	75.86	77.19	79.31	81.48	80.77	82.69	100	50.82	52.46	49.12	56.86	53.85	15.38	10.14	5.33	3.03
RcTitan	53.45	56.14	55.17	57.41	61.54	59.62	56.36	100	95.08	45.61	49.02	50	14.29	8.7	9.33	3.03
RcSpartan	50	52.63	51.72	53.7	57.69	57.69	58.18	95.08	100	45.61	49.02	50	14.29	8.7	9.33	3.03
IME_AB3	53.45	54.39	53.45	53.7	59.62	55.77	52.73	42.62	42.62	100	84.31	46.15	19.78	8.7	1.33	1.52
Loki	50	52.63	51.72	51.85	57.69	55.76	52.73	40.98	40.98	75.44	100	46.15	19.78	10.14	1.33	1.52
IMEP1	43.1	45.61	43.1	44.44	48.08	48.08	49.09	42.62	42.62	42.11	47.06	100	15.38	11.59	5.33	1.52
Cajan	20.69	22.81	20.69	24.07	25	25	23.64	22.95	21.31	31.58	35.29	23.08	100	13.04	5.33	4.55
Jersey	10.34	10.53	10.34	11.1	11.54	11.54	12.73	9.84	11.48	10.53	13.73	15.38	9.89	100	8	4.55
Chi	8.62	7.02	6.9	7.41	7.69	9.62	7.27	11.48	11.48	1.75	1.96	7.69	4.4	8.7	100	12.12
Lambda	1.72	3.51	1.72	3.7	1.92	1.92	3.64	3.28	3.28	1.75	1.96	1.92	4.4	2.9	10.67	100

**Fig 5.** (a) Phylogenetic tree of co-linearised whole genome nucleotide sequences of Loki and phages linked by TBLASTX searches. The neighbour joining tree was constructed using ClustalX with 1,000 bootstrap replicates. The scale bar represents substitutions per site. (b) Percent nucleotide identity matrix determined using EMBOSS Stretcher. (c) Matrix showing the percentage of shared genes determined using CoreGenes 3.5. Cells are coloured from green to red to show increasing similarity. Phages Jersey, Lambda, Cajan and Chi were included as outliers.

doi:10.1371/journal.pone.0172303.g005

Each of the phages linked by TBLASTX possess a similar genome size (41.3 to 43.1 kb) and number of ORFs (51 to 58). Each phage exhibits conservation of structural genes encoding the DNA packaging apparatus, virion head and tail but possess distinct genes encoding the tail tip complex and adsorption apparatus reflecting their different host tropism. Key

replicative gene products including a DNA polymerase, helicase, primase, single stranded DNA binding protein and MazG are also conserved between the phages. The gene products encoded within the early/lysis gene module are significantly more divergent, with only the putative holin conserved in each phage. The EMBOSS stretcher and CoreGenes data suggest that KL1, SCH\_Ab2, Kakheti25, PS9N, PA73, DLP\_1 and DLP\_2 represent a discrete clade of *Siphoviridae* united by a minimum 67.1% sequence identity and 75.9% shared orthologous proteins. This cluster of phages are more distantly related to Loki and IME\_AB3; the two groups are linked by a minimum of 50% nucleotide sequence identity and 49% protein homologs.

### 3 Discussion

The reduction in cost of genome sequencing has led to a marked increase in the number of complete phage genomes deposited in the international sequence databases (EMBL, GenBank and DDBJ). This wealth of sequence data has demonstrated the enormous diversity of the tailed phages and led to the proposal of new taxonomic relationships between phages isolated at disparate times and geographic locations. Significant work has recently been reported defining taxonomic relationships within the *Siphoviridae* and for bacteriophages infecting the Enterobacteriaceae [48–50]. In contrast to phages infecting other Gram-negative bacteria, particularly those infecting genera of the Enterobacteriaceae, few *Acinetobacter* phages have been sequenced.

Loki and IME\_AB3 are two closely related representatives of a novel group of siphoviruses known to infect *A. baumannii* that exhibit little nucleotide similarity to other *Siphoviridae* in the extant sequence databases. However, the analysis of gene products demonstrates that these two *Acinetobacter* phages share a significant number of genes involved in virion morphogenesis and DNA replication with a small group of phages infecting *Pseudomonas*, *Paracoccus*, *Burkholderia* and *Rhodobacter* species. Loki and IME\_AB3 are distinguished primarily by the presence of different small hypothetical proteins situated in the early/lysis gene module. Due to the lack of functional inferences that could be obtained using bioinformatics approaches and from the genomic location we posit that these proteins might be expressed early in infection and be involved in the hijack of host cell functions. A second distinguishing feature is the structure of the endolysin. In Loki the endolysin is modular, comprising a conserved peptidoglycan-binding domain and an N-acetylmuraminidase domain. In contrast the endolysin encoded by IME\_AB3 is predicted to encode a single glycoside hydrolase family 19 domain.

A common feature of bacteriophage genomes is the presence of small genes of unknown function, many of which exhibit little or no similarity to entries in the extant sequence database [51]. The establishment of a productive lytic infection depends upon the interaction between phage- and host-encoded proteins in order to inhibit, regulate and/or subvert a variety of cellular processes to create an optimal environment for the production of progeny virions [52]. Recent work on bacteriophages infecting *Pseudomonas aeruginosa* has leveraged RNA sequencing, protein-protein interaction and metabolomics studies to identify proteins expressed early in infection involved in host cell takeover [53–56]. These studies have revealed a number of inhibitory phage proteins that target an array of host cellular processes including transcription, RNA degradation, DNA replication, cell division and fatty acid and riboflavin biosynthesis pathways. Such genome mining approaches are important not only for the elucidation of bacteriophage biology but also to leverage rational drug design by mimicking the mechanism of action of antibacterial phage proteins in an era where the rate of discovery of new antibiotics has slowed and antibiotic resistance is increasing. Given the prevalence and breadth of antimicrobial resistance in *A. baumannii*, similar approaches are required to elucidate the biological mechanisms underlying productive phage infection.

## 4 Materials and methods

### 4.1 Bacteriophage isolation and purification

In June 2015 a fresh sample of approximately 500 ml of activated sludge from Cam Valley sewage treatment works was provided by Wessex Water Services Ltd. Bacteriophage Loki was isolated by incubation of 5 ml of activated sludge diluted in 5 ml of double-strength LB broth (Invitrogen, UK) supplemented with 10 mmol l<sup>-1</sup> MgSO<sub>4</sub> and 5 mmol l<sup>-1</sup> CaCl<sub>2</sub>. A 200 µl volume of an overnight batch culture of *A. baumannii* ATCC 17978 was added and the enrichment sample was incubated at 30°C for 18 hours with shaking at 150 rpm. Following incubation, the enrichment sample was centrifuged (8,000 x g, 10 minutes) to pellet bacterial cells, filtered (0.45 µm pore size) and assessed for the presence of bacteriophage by overlay plaque assay [57]. Clonal preparations were made by stab sampling an individual plaque followed by elution in SM buffer and plating on overlay agar.

High titre phage stocks were prepared by broth lysis. In brief, host bacteria were grown in LB broth at 30°C with orbital shaking at 150 rpm to an OD<sub>600nm</sub> of 0.1 (c. 5 x 10<sup>7</sup> c.f.u. ml<sup>-1</sup>). Bacteriophages were added to yield a multiplicity of infection of 0.1 and subsequent growth and lysis of cultures was monitored by measurements of optical density at 30 minute intervals. Residual bacteria were killed by the addition of chloroform (final concentration of 1% v/v) and the crude lysates were treated with DNase I and RNase A (Sigma Aldrich, UK) at final concentrations of 1 µg ml<sup>-1</sup> for 1 hour at 37°C prior to the removal of bacterial debris by centrifugation at 11,000 x g for 10 min at 4°C. The supernatant was filtered (0.2 µm pore size) and bacteriophages precipitated by addition of PEG 8000 (10% W/V) and 1 mol l<sup>-1</sup> NaCl [58]. Precipitated phages were recovered by centrifugation at 11,000 x g for 20 minutes and residual PEG was removed by centrifugation with an equal volume of chloroform at 3,000 x g for 10 minutes. Pure preparations of bacteriophages were obtained by isopycnic centrifugation using a SW40Ti rotor (Beckman Coulter, UK) at 160,000 x g for 24 hours at 4°C in 0.75 g ml<sup>-1</sup> cesium chloride. Following centrifugation, bands (approximately 1 ml) were recovered using a syringe and dialysed using a 10 kDa dialysis cassette (Thermo Fisher Scientific, UK) against two 500-fold volume changes of SM buffer to remove residual CsCl and stored at 4°C in SM buffer (50 mmol l<sup>-1</sup> Tris, 100 mmol l<sup>-1</sup> NaCl, 8 mmol l<sup>-1</sup> MgSO<sub>4</sub>, pH7.5).

### 4.2 Electron microscopy

Transmission electron microscopy was performed as described previously [59]. CsCl-purified bacteriophages were pelleted by centrifugation at 25,000 x g for 1 hour and washed in 0.1 M ammonium acetate (pH 7.2; Sigma-Aldrich, UK). Samples were deposited on 200 mesh formvar carbon-coated grids (Agar Scientific, UK) and stained with either 1% (w/v) uranyl acetate solution (pH 4.5; Sigma-Aldrich, UK) or 2% (w/v) sodium phosphotungstate (pH 7.0; Sigma-Aldrich, UK). All specimens were examined using a Philips CM10 transmission electron microscope operated at 60 kV. Magnification was calibrated using T4 tails and virion dimensions established by measurement of 20 intact particles.

### 4.3 Adsorption and one-step growth

Phage adsorption to host cells was performed as described previously [57]. Host strains were grown in LB to an OD<sub>600nm</sub> of 0.1 (approx. 5 x 10<sup>7</sup> c.f.u. ml<sup>-1</sup>), serially diluted and enumerated using a spiral plating system (Don Whately Scientific, UK). Bacteriophages were added to cultures to yield a final concentration of 5 x 10<sup>4</sup> p.f.u. ml<sup>-1</sup> (t = 0). At 1 min intervals, 50 µl was transferred to 950 µl SM buffer saturated with chloroform and stored on ice. Samples were titrated for unabsorbed bacteriophages by triplicate overlay plaque assays. Absorption rate



constants ( $k$ ) were calculated as  $-m/N$ , where  $m$  represents the slope of linear regression of the natural logarithm of the free phage titre over time and  $N$  the initial bacterial density in c.f.u.  $\text{ml}^{-1}$ .

For one-step growth experiments, bacteriophages were added to host bacteria at a multiplicity of infection of 0.05 and allowed to adsorb for 5 minutes, then centrifuged at  $13,000 \times g$  for 1 min. The supernatant containing unabsorbed bacteriophages was discarded and the pellet resuspended in 10 ml of fresh LB broth, diluted to  $10^{-2}$  and incubated at  $30^\circ\text{C}$ . Samples were taken at 5 minute intervals over a 2-hour period and titrated by triplicate overlay plaque assays. Infected cultures for single burst experiments were prepared in the same way, diluted to  $10^{-7}$  and 0.5 ml aliquots distributed to 50 tubes. After incubation for 2 hours at  $30^\circ\text{C}$  plaque overlay plates were prepared using the entire volume from each tube. The expected number of infected cells was calculated using the Poisson distribution from the observed number of plates yielding no plaques. For the three independent repeats the expected number of cells were 11, 5 and 6, equivalent to 0.22, 0.11 and 0.13 infected cells per 0.5 ml aliquot.

#### 4.4 Determination of host range

Bacteriophage host range and efficiency of plating (EOP) were determined by the standard double agar layer plating technique [60]. Prior to testing, bacteriophages were adjusted by dilution to yield a titre of  $10^{10}$  p.f.u.  $\text{ml}^{-1}$  on their respective propagating host. Spot tests were performed using square 120 mm plates (Greiner BioOne, UK) containing LB agar were subdivided to yield a  $6 \times 6$  grid, to which 8 ml LB overlay agar containing 200  $\mu\text{l}$  of an exponential phase culture was overlaid. To each section of the grid, 5  $\mu\text{l}$  aliquots of bacteriophage from a tenfold dilution series were spotted onto the surface of the overlay agar so that each plate assessed a range of phage concentrations ( $10^{10}$  to  $10^3$  p.f.u.  $\text{ml}^{-1}$ ). Phage samples were allowed to absorb into the overlay agar prior to incubation at  $30^\circ\text{C}$  and examined for plaque formation after 24 hours. For EOP testing, overlay plaque assay plates were prepared containing 10  $\mu\text{l}$  of serial dilutions of bacteriophage and 150  $\mu\text{l}$  of exponential phase bacterial cultures. Following overnight incubation at  $30^\circ\text{C}$ , the relative EOP was expressed as the ratio between the titre in p.f.u.  $\text{ml}^{-1}$  for a given isolate and the titre for the propagating host from overlay plaque assays.

#### 4.5 DNA electrophoresis

Genome size was estimated by pulsed-field gel electrophoresis. Agarose plugs (1% w/v agarose) were prepared containing bacteriophages at an approximate concentration of  $1 \times 10^8$  pfu  $\text{ml}^{-1}$  and lysed by addition of proteinase K (New England Biolabs, UK) and SDS to final concentrations of 50  $\mu\text{g ml}^{-1}$  and 0.5% w/v, respectively, in 10 mM Tris, 50 mM EDTA and incubating for 2 hours at  $54^\circ\text{C}$ . Agarose plugs were washed three times by soaking in Tris-EDTA buffer (10 mM Tris, 1 mM EDTA; Sigma Aldrich, UK) for 1 hour. Gels (1% w/v agarose in 0.5x Tris Borate EDTA (TBE) buffer) were run at  $6 \text{ V cm}^{-1}$  for 14 hours in 0.5x TBE buffer at  $15^\circ\text{C}$  with pulses of 1 to 12 seconds using a CHEF DRII electrophoresis unit (BioRad, France). DNA size standards were provided by a low-range PFGE ladder (New England Biolabs, UK).

Restriction digests of phage genomic DNA were separated using either 0.8% w/v agarose gels run at  $4.5 \text{ V cm}^{-1}$  or 0.6% w/v agarose gels at  $3.5 \text{ V cm}^{-1}$  in 1x TAE buffer (pH 8.0) as appropriate. DNA size standards were provided using 2-log and 1 kb extend DNA ladders (New England Biolabs, UK). Bands were visualised by staining with SYBR Safe (Life Sciences, UK) and gels imaged using a FluorChem Q (ProteinSimple, UK) and analysed using ImageJ [61].

#### 4.6 1D SDS-PAGE

Virion structural proteins were concentrated using methanol-chloroform extraction [62] from CsCl-purified samples. Extracted proteins were suspended in lithium dodecyl sulphate sample

buffer (Invitrogen) prior to heating at 70°C for 10 minutes. Protein separation was performed using a NuPAGE mini-gel system and Novex 4–12% Bis-Tris gels in MES–SDS running buffer at 200 V alongside Novex Sharp unstained protein standards (Life Technologies, UK). SDS-PAGE gels were stained using SimplyBlue Safestain (Life Technologies, UK).

#### 4.7 Genome sequencing and bioinformatics

Bacteriophage genomic DNA was isolated by phenol:chloroform extraction [58]. Sequencing was performed using the Illumina MiSeq platform (Illumina Inc., USA) at the Nucleomics Core (VIB, Belgium). A custom 2\*150 bp paired-end DNA library (Nextera XT sample prep) was prepared with an average fragment length of 500 bp. The quality of each library preparation was verified using the Agilent Bioanalyzer. The library prep was sequenced and reads containing adapters, contamination or low-quality bases were removed in the pre-processing step. Quality trimming of the paired-end data set was performed with CLC Bio Genomics Workbench v7.0 (Aarhus, Denmark) using a quality score of 0.02 and a maximum of 2 ambiguous nucleotides per read. Next, *de novo* assembly was performed with the trimmed paired-end dataset with word and bubble size set at 20 and 50, respectively, a minimum contig length of 200 bp and auto detection of paired distances with scaffolding. This resulted in a single contig with an average coverage of 3,435 x. The assembly was circular with a relatively homogenous coverage.

Bioinformatics analysis was performed on the Biolinux 8 operating system [63]. Open reading frames (ORFs) were predicted using a combination of GeneMark [64], Glimmer 3.02 [65] and Prodigal [66]. Annotation was performed using Artemis [67] and graphical maps were prepared using the CGView Comparison Tool [29]. Nucleotide sequences were queried against the non-redundant database using standard and discontinuous megablast. Putative functions for gene products were assigned by querying translated sequences using BLASTP and PSI-BLAST against the non-redundant database [68,69] and by searches against the conserved domain database [70], Pfam [71] and InterPro [72]. Additional functional inferences were obtained using the HH-suite toolset [73,74]. The ExPASy tool Compute pI/Mw [75] was used to predict molecular weight and isoelectric point. Prediction of trans-membrane helices was performed using TMHMM 2.0 [76] and searches for signal peptides were carried out using SignalP [77]. tRNAScan-SE [78] and ARAGORN [79] were used to predict of tRNAs. Searches for regulatory elements, candidate promoter sequences and conserved intergenic motifs were performed using MEME on 100 bp sequences upstream of ORFs [80]. Putative rho-independent terminators were predicted using TransTermHP [81] and candidate terminators were assessed according to location, the presence of a U-rich tail and stable predicted stem loop secondary structure ( $\Delta G \leq -10 \text{ kcal mol}^{-1}$ ) as calculated by MFold [82].

### Supporting information

**S1 File. Restriction digests of *Acinetobacter* bacteriophage Loki DNA.**

(PDF)

**S2 File. Features, BLASTP homologues and presence of conserved domains and motifs of predicted proteins encoded by *Acinetobacter* bacteriophage Loki.**

(XLSX)

**S1 Table. *Acinetobacter* spp. assessed by spot plate assay and efficiency of plating (EOP).**

(PDF)

## Acknowledgments

This work was supported by a QR2015 award from the University of the West of England, Bristol. R.L. is supported by a the Geconcerteerde Onderzoeks Actie grant ‘Phage Biosystems’ from KU Leuven. R.L. & Y.B. are members of the FWO research community ‘Phagebiotics’. The funders had no role in study design, data collection and interpretation, or the decision to submit the work for publication. We wish to thank Dr J. Turton (Public Health England) and Dr D. Centron (Universidad de Buenos Aires-Consejo Nacional de Investigaciones Científicas y Tecnológicas) for the supply and permission to use bacterial strains, and Wessex Water PLC for the provision of sewage and activated sludge samples. We thank Professor H.-W. Ackermann (Université Laval) for his advice and informative discussions on the bacteriophages of *Acinetobacter* sp.

## Author Contributions

**Conceptualization:** DT DMR JMS.

**Investigation:** DT MEW YB.

**Resources:** DT DMR JMS MEW YB RL.

**Writing – original draft:** DT DMR JMS MEW YB RL.

## References

1. Ackermann HW, Prangishvili D (2012) Prokaryote viruses studied by electron microscopy. *Archives of Virology* 157: 1843–1849. doi: [10.1007/s00705-012-1383-y](https://doi.org/10.1007/s00705-012-1383-y) PMID: [22752841](https://pubmed.ncbi.nlm.nih.gov/22752841/)
2. Jeon J, D'Souza R, Pinto N, Ryu C-M, Park J-h, Yong D, et al. (2015) Complete genome sequence of the siphoviral bacteriophage Bφ-R3177, which lyses an OXA-66-producing carbapenem-resistant *Acinetobacter baumannii* isolate. *Archives of Virology* 160: 3157–3160. doi: [10.1007/s00705-015-2604-y](https://doi.org/10.1007/s00705-015-2604-y) PMID: [26427378](https://pubmed.ncbi.nlm.nih.gov/26427378/)
3. Jeon J, Kim J-w, Yong D, Lee K, Chong Y (2012) Complete Genome Sequence of the Podoviral Bacteriophage YMC/09/02/B1251 ABA BP, Which Causes the Lysis of an OXA-23-Producing Carbapenem-Resistant *Acinetobacter baumannii* Isolate from a Septic Patient. *Journal of Virology* 86: 12437–12438. doi: [10.1128/JVI.02132-12](https://doi.org/10.1128/JVI.02132-12) PMID: [23087105](https://pubmed.ncbi.nlm.nih.gov/23087105/)
4. Turner D, Wand ME, Sutton JM, Centron D, Kropinski AM, Reynolds D (2016) Genome sequence of vB\_AbaS\_TRS1, a viable prophage isolated from *Acinetobacter baumannii* strain A118. *Genome Announcements* 4: e01051–16 doi: [10.1128/genomeA.01051-16](https://doi.org/10.1128/genomeA.01051-16) PMID: [27738026](https://pubmed.ncbi.nlm.nih.gov/27738026/)
5. Dijkshoorn L, Nemeč A, Seifert H (2007) An increasing threat in hospitals: multidrug-resistant *Acinetobacter baumannii*. *Nature Reviews Microbiology* 5: 939–951. doi: [10.1038/nrmicro1789](https://doi.org/10.1038/nrmicro1789) PMID: [18007677](https://pubmed.ncbi.nlm.nih.gov/18007677/)
6. Wendt C, Dietze B, Dietz E, Rüdén H (1997) Survival of *Acinetobacter baumannii* on dry surfaces. *Journal of Clinical Microbiology* 35: 1394–1397. PMID: [9163451](https://pubmed.ncbi.nlm.nih.gov/9163451/)
7. Wisplinghoff H, Schmitt R, Wöhrmann A, Stefanik D, Seifert H (2007) Resistance to disinfectants in epidemiologically defined clinical isolates of *Acinetobacter baumannii*. *Journal of Hospital Infection* 66: 174–181. doi: [10.1016/j.jhin.2007.02.016](https://doi.org/10.1016/j.jhin.2007.02.016) PMID: [17498843](https://pubmed.ncbi.nlm.nih.gov/17498843/)
8. Poirel L, Bonnin RA, Nordmann P (2011) Genetic basis of antibiotic resistance in pathogenic *Acinetobacter* species. *IUBMB Life* 63: 1061–1067. doi: [10.1002/iub.532](https://doi.org/10.1002/iub.532) PMID: [21990280](https://pubmed.ncbi.nlm.nih.gov/21990280/)
9. Perez F, Hujer AM, Hujer KM, Decker BK, Rather PN, Bonomo RA (2007) Global challenge of multidrug-resistant *Acinetobacter baumannii*. *Antimicrobial Agents and Chemotherapy* 51: 3471–3484. doi: [10.1128/AAC.01464-06](https://doi.org/10.1128/AAC.01464-06) PMID: [17646423](https://pubmed.ncbi.nlm.nih.gov/17646423/)
10. Cai Y, Chai D, Wang R, Liang B, Bai N (2012) Colistin resistance of *Acinetobacter baumannii*: clinical reports, mechanisms and antimicrobial strategies. *Journal of Antimicrobial Chemotherapy* 67: 1607–1615. doi: [10.1093/jac/dks084](https://doi.org/10.1093/jac/dks084) PMID: [22441575](https://pubmed.ncbi.nlm.nih.gov/22441575/)
11. Wand ME, Bock LJ, Bonney LC, Sutton JM (2015) Retention of virulence following adaptation to colistin in *Acinetobacter baumannii* reflects the mechanism of resistance. *Journal of Antimicrobial Chemotherapy* 70: 2209–2216. doi: [10.1093/jac/dkv097](https://doi.org/10.1093/jac/dkv097) PMID: [25904728](https://pubmed.ncbi.nlm.nih.gov/25904728/)

12. Lynch K, Stothard P, Dennis J (2012) Comparative analysis of two phenotypically-similar but genomically-distinct *Burkholderia cenocepacia*-specific bacteriophages. *BMC Genomics* 13: 223. doi: [10.1186/1471-2164-13-223](https://doi.org/10.1186/1471-2164-13-223) PMID: [22676492](https://pubmed.ncbi.nlm.nih.gov/22676492/)
13. Moffatt JH, Harper M, Harrison P, Hale JDF, Vinogradov E, Seemann T, et al. (2010) Colistin resistance in *Acinetobacter baumannii* is mediated by complete loss of lipopolysaccharide production. *Antimicrobial Agents and Chemotherapy* 54: 4971–4977. doi: [10.1128/AAC.00834-10](https://doi.org/10.1128/AAC.00834-10) PMID: [20855724](https://pubmed.ncbi.nlm.nih.gov/20855724/)
14. Geisinger E, Isberg RR (2015) Antibiotic modulation of capsular exopolysaccharide and virulence in *Acinetobacter baumannii*. *PLOS Pathogens* 11: e1004691. doi: [10.1371/journal.ppat.1004691](https://doi.org/10.1371/journal.ppat.1004691) PMID: [25679516](https://pubmed.ncbi.nlm.nih.gov/25679516/)
15. Rakhuba DV, Kolomiets EI, Dey ES, Novik GI (2010) Bacteriophage receptors, mechanisms of phage adsorption and penetration into host cell. *Polish Journal of Microbiology* 59: 145–155. PMID: [21033576](https://pubmed.ncbi.nlm.nih.gov/21033576/)
16. Shin H, Lee JH, Kim H, Choi Y, Heu S, Ryu S (2012) Receptor diversity and host interaction of bacteriophages infecting *Salmonella enterica* serovar Typhimurium. *PLoS One* 7: e43392. doi: [10.1371/journal.pone.0043392](https://doi.org/10.1371/journal.pone.0043392) PMID: [22927964](https://pubmed.ncbi.nlm.nih.gov/22927964/)
17. Fullner KJ, Hatfull GF (1997) Mycobacteriophage L5 infection of *Mycobacterium bovis* BCG: implications for phage genetics in the slow-growing mycobacteria. *Molecular Microbiology* 26: 755–766. PMID: [9427405](https://pubmed.ncbi.nlm.nih.gov/9427405/)
18. Bonhivers M, Letellier L (1995) Calcium controls phage T5 infection at the level of the *Escherichia coli* cytoplasmic membrane. *FEBS Letters* 374: 169–173. PMID: [7589527](https://pubmed.ncbi.nlm.nih.gov/7589527/)
19. Steensma HY, Blok J (1979) Effect of Calcium Ions on the Infection of *Bacillus subtilis* by Bacteriophage SF 6. *Journal of General Virology* 42: 305–314. doi: [10.1099/0022-1317-42-2-305](https://doi.org/10.1099/0022-1317-42-2-305) PMID: [106092](https://pubmed.ncbi.nlm.nih.gov/106092/)
20. Mahony J, Tremblay DM, Labrie SJ, Moineau S, van Sinderen D (2015) Investigating the requirement for calcium during lactococcal phage infection. *International Journal of Food Microbiology* 201: 47–51. doi: [10.1016/j.ijfoodmicro.2015.02.017](https://doi.org/10.1016/j.ijfoodmicro.2015.02.017) PMID: [25744695](https://pubmed.ncbi.nlm.nih.gov/25744695/)
21. Abedon ST (2011) Lysis from without. *Bacteriophage* 1: 46–49. doi: [10.4161/bact.1.1.13980](https://doi.org/10.4161/bact.1.1.13980) PMID: [21687534](https://pubmed.ncbi.nlm.nih.gov/21687534/)
22. Andrews HJ (1986) *Acinetobacter* bacteriocin typing. *Journal of Hospital Infection* 7: 169–175. PMID: [2871080](https://pubmed.ncbi.nlm.nih.gov/2871080/)
23. Labrie SJ, Samson JE, Moineau S (2010) Bacteriophage resistance mechanisms. *Nature Reviews Microbiology* 8: 317–327. doi: [10.1038/nrmicro2315](https://doi.org/10.1038/nrmicro2315) PMID: [20348932](https://pubmed.ncbi.nlm.nih.gov/20348932/)
24. Casjens SR, Gilcrease EB (2009) Determining DNA packaging strategy by analysis of the termini of the chromosomes in tailed-bacteriophage virions. *Methods in Molecular Biology* 502: 91–111. doi: [10.1007/978-1-60327-565-1\\_7](https://doi.org/10.1007/978-1-60327-565-1_7) PMID: [19082553](https://pubmed.ncbi.nlm.nih.gov/19082553/)
25. Merrill BD, Ward AT, Grose JH, Hope S (2016) Software-based analysis of bacteriophage genomes, physical ends, and packaging strategies. *BMC Genomics* 17: 679. doi: [10.1186/s12864-016-3018-2](https://doi.org/10.1186/s12864-016-3018-2) PMID: [27561606](https://pubmed.ncbi.nlm.nih.gov/27561606/)
26. Loessner MJ, Inman RB, Lauer P, Calendar R (2000) Complete nucleotide sequence, molecular analysis and genome structure of bacteriophage A118 of *Listeria monocytogenes*: implications for phage evolution. *Molecular Microbiology* 35: 324–340. PMID: [10652093](https://pubmed.ncbi.nlm.nih.gov/10652093/)
27. Casjens SR (2005) Comparative genomics and evolution of the tailed-bacteriophages. *Current Opinion in Microbiology* 8: 451–458. doi: [10.1016/j.mib.2005.06.014](https://doi.org/10.1016/j.mib.2005.06.014) PMID: [16019256](https://pubmed.ncbi.nlm.nih.gov/16019256/)
28. Hatfull GF (2008) Bacteriophage genomics. *Current Opinion in Microbiology* 11: 447–453. doi: [10.1016/j.mib.2008.09.004](https://doi.org/10.1016/j.mib.2008.09.004) PMID: [18824125](https://pubmed.ncbi.nlm.nih.gov/18824125/)
29. Grant J, Arantes A, Stothard P (2012) Comparing thousands of circular genomes using the CGView Comparison Tool. *BMC Genomics* 13: 202. doi: [10.1186/1471-2164-13-202](https://doi.org/10.1186/1471-2164-13-202) PMID: [22621371](https://pubmed.ncbi.nlm.nih.gov/22621371/)
30. Cardarelli L, Lam R, Tuite A, Baker LA, Sadowski PD, Radford DR, et al. (2010) The crystal structure of bacteriophage HK97 gp6: defining a large family of head-tail connector proteins. *Journal of Molecular Biology* 395: 754–768. doi: [10.1016/j.jmb.2009.10.067](https://doi.org/10.1016/j.jmb.2009.10.067) PMID: [19895817](https://pubmed.ncbi.nlm.nih.gov/19895817/)
31. Maxwell KL, Yee AA, Arrowsmith CH, Gold M, Davidson AR (2002) The solution structure of the bacteriophage lambda head-tail joining protein, gpFII. *Journal of Molecular Biology* 318: 1395–1404. PMID: [12083526](https://pubmed.ncbi.nlm.nih.gov/12083526/)
32. Chagot B, Auzat I, Gallopin M, Petitpas I, Gilquin B, Tavares P, et al. (2012) Solution structure of gp17 from the *Siphoviridae* bacteriophage SPP1: insights into its role in virion assembly. *Proteins* 80: 319–326. doi: [10.1002/prot.23191](https://doi.org/10.1002/prot.23191) PMID: [22072538](https://pubmed.ncbi.nlm.nih.gov/22072538/)
33. Pell LG, Liu A, Edmonds L, Donaldson LW, Howell PL, Davidson AR (2009) The X-ray crystal structure of the phage lambda tail terminator protein reveals the biologically relevant hexameric ring structure and demonstrates a conserved mechanism of tail termination among diverse long-tailed phages. *Journal of Molecular Biology* 389: 938–951. doi: [10.1016/j.jmb.2009.04.072](https://doi.org/10.1016/j.jmb.2009.04.072) PMID: [19426744](https://pubmed.ncbi.nlm.nih.gov/19426744/)



34. Christie GE, Temple LM, Bartlett BA, Goodwin TS (2002) Programmed translational frameshift in the bacteriophage P2 FETUD tail gene operon. *Journal of Bacteriology* 184: 6522–6531. doi: [10.1128/JB.184.23.6522-6531.2002](https://doi.org/10.1128/JB.184.23.6522-6531.2002) PMID: [12426340](https://pubmed.ncbi.nlm.nih.gov/12426340/)
35. Levin ME, Hendrix RW, Casjens SR (1993) A programmed translational frameshift is required for the synthesis of a bacteriophage  $\lambda$  tail assembly protein. *Journal of Molecular Biology* 234: 124–139. doi: [10.1006/jmbi.1993.1568](https://doi.org/10.1006/jmbi.1993.1568) PMID: [8230192](https://pubmed.ncbi.nlm.nih.gov/8230192/)
36. Pell LG, Cumby N, Clark TE, Tuite A, Battaile KP, Edwards AM, et al. (2013) A conserved spiral structure for highly diverged phage tail assembly chaperones. *Journal of Molecular Biology* 425: 2436–2449. doi: [10.1016/j.jmb.2013.03.035](https://doi.org/10.1016/j.jmb.2013.03.035) PMID: [23542344](https://pubmed.ncbi.nlm.nih.gov/23542344/)
37. Xu J, Hendrix RW, Duda RL (2004) Conserved translational frameshift in dsDNA bacteriophage tail assembly genes. *Molecular Cell* 16: 11–21. doi: [10.1016/j.molcel.2004.09.006](https://doi.org/10.1016/j.molcel.2004.09.006) PMID: [15469818](https://pubmed.ncbi.nlm.nih.gov/15469818/)
38. Flayhan A, Vellieux FMD, Lurz R, Maury O, Contreras-Martel C, Girard E, et al. (2014) Crystal structure of pb9, the distal tail protein of bacteriophage T5: a conserved structural motif among all siphophages. *Journal of Virology* 88: 820–828. doi: [10.1128/JVI.02135-13](https://doi.org/10.1128/JVI.02135-13) PMID: [24155371](https://pubmed.ncbi.nlm.nih.gov/24155371/)
39. Zhang J, Inouye M (2002) MazG, a nucleoside triphosphate pyrophosphohydrolase, interacts with Era, an essential GTPase in *Escherichia coli*. *Journal of Bacteriology* 184: 5323–5329. doi: [10.1128/JB.184.19.5323-5329.2002](https://doi.org/10.1128/JB.184.19.5323-5329.2002) PMID: [12218018](https://pubmed.ncbi.nlm.nih.gov/12218018/)
40. Angly F, Youle M, Nosrat B, Srinagesh S, Rodriguez-Brito B, McNairnie P, et al. (2009) Genomic analysis of multiple Roseophage SIO1 strains. *Environmental Microbiology* 11: 2863–2873. doi: [10.1111/j.1462-2920.2009.02021.x](https://doi.org/10.1111/j.1462-2920.2009.02021.x) PMID: [19659499](https://pubmed.ncbi.nlm.nih.gov/19659499/)
41. Bryan MJ, Burroughs NJ, Spence EM, Clokie MRJ, Mann NH, Bryan SJ (2008) Evidence for the intense exchange of MazG in marine cyanophages by horizontal gene transfer. *PLoS ONE* 3: e2048. doi: [10.1371/journal.pone.0002048](https://doi.org/10.1371/journal.pone.0002048) PMID: [18431505](https://pubmed.ncbi.nlm.nih.gov/18431505/)
42. Weigle PR, Pope WH, Pedulla ML, Houtz JM, Smith AL, Conway JF, et al. (2007) Genomic and structural analysis of Syn9, a cyanophage infecting marine *Prochlorococcus* and *Synechococcus*. *Environmental Microbiology* 9: 1675–1695. doi: [10.1111/j.1462-2920.2007.01285.x](https://doi.org/10.1111/j.1462-2920.2007.01285.x) PMID: [17564603](https://pubmed.ncbi.nlm.nih.gov/17564603/)
43. Peters D, Lynch K, Stothard P, Dennis J (2015) The isolation and characterization of two *Stenotrophomonas maltophilia* bacteriophages capable of cross-taxonomic order infectivity. *BMC Genomics* 16: 664. doi: [10.1186/s12864-015-1848-y](https://doi.org/10.1186/s12864-015-1848-y) PMID: [26335566](https://pubmed.ncbi.nlm.nih.gov/26335566/)
44. Briers Y, Volckaert G, Cornelissen A, Lagaert S, Michiels CW, Hertveldt K, et al. (2007) Muralytic activity and modular structure of the endolysins of *Pseudomonas aeruginosa* bacteriophages  $\phi$ KZ and EL. *Molecular Microbiology* 65: 1334–1344. doi: [10.1111/j.1365-2958.2007.05870.x](https://doi.org/10.1111/j.1365-2958.2007.05870.x) PMID: [17697255](https://pubmed.ncbi.nlm.nih.gov/17697255/)
45. Bollivar DW, Bernardoni B, Bockman MR, Miller BM, Russell DA, Delesalle VA, et al. (2016) Complete genome sequences of five bacteriophages that infect *Rhodobacter capsulatus*. *Genome Announcements* 4.
46. Karumidze N, Thomas JA, Kvatadze N, Goderdzishvili M, Hakala K, Weintraub ST, et al. (2012) Characterization of lytic *Pseudomonas aeruginosa* bacteriophages via biological properties and genomic sequences. *Applied Microbiology and Biotechnology* 94: 1609–1617. doi: [10.1007/s00253-012-4119-8](https://doi.org/10.1007/s00253-012-4119-8) PMID: [22562168](https://pubmed.ncbi.nlm.nih.gov/22562168/)
47. Kwan T, Liu J, DuBow M, Gros P, Pelletier J (2006) Comparative genomic analysis of 18 *Pseudomonas aeruginosa* bacteriophages. *Journal of Bacteriology* 188: 1184–1187. doi: [10.1128/JB.188.3.1184-1187.2006](https://doi.org/10.1128/JB.188.3.1184-1187.2006) PMID: [16428425](https://pubmed.ncbi.nlm.nih.gov/16428425/)
48. Adriaenssens EM, Edwards R, Nash JHE, Mahadevan P, Seto D, Ackermann H-W, et al. (2015) Integration of genomic and proteomic analyses in the classification of the Siphoviridae family. *Virology* 477: 144–154. doi: [10.1016/j.virol.2014.10.016](https://doi.org/10.1016/j.virol.2014.10.016) PMID: [25466308](https://pubmed.ncbi.nlm.nih.gov/25466308/)
49. Grose JH, Casjens SR (2014) Understanding the enormous diversity of bacteriophages: The tailed phages that infect the bacterial family Enterobacteriaceae. *Virology* 468–470: 421–443. doi: [10.1016/j.virol.2014.08.024](https://doi.org/10.1016/j.virol.2014.08.024) PMID: [25240328](https://pubmed.ncbi.nlm.nih.gov/25240328/)
50. Adams MJ, Lefkowitz EJ, King AMQ, Bamford DH, Breitbart M, Davison AJ, et al. (2015) Ratification vote on taxonomic proposals to the International Committee on Taxonomy of Viruses (2015). *Archives of Virology* 160: 1837–1850. doi: [10.1007/s00705-015-2425-z](https://doi.org/10.1007/s00705-015-2425-z) PMID: [25913692](https://pubmed.ncbi.nlm.nih.gov/25913692/)
51. Hatfull GF (2015) Dark matter of the biosphere: the amazing world of bacteriophage diversity. *Journal of Virology* 89: 8107–8110. doi: [10.1128/JVI.01340-15](https://doi.org/10.1128/JVI.01340-15) PMID: [26018169](https://pubmed.ncbi.nlm.nih.gov/26018169/)
52. Roucourt B, Lavigne R (2009) The role of interactions between phage and bacterial proteins within the infected cell: a diverse and puzzling interactome. *Environmental Microbiology* 11: 2789–2805. doi: [10.1111/j.1462-2920.2009.02029.x](https://doi.org/10.1111/j.1462-2920.2009.02029.x) PMID: [19691505](https://pubmed.ncbi.nlm.nih.gov/19691505/)
53. Van den Bossche A, Ceysens P-J, De Smet J, Hendrix H, Bellon H, Leimer N, et al. (2014) Systematic Identification of Hypothetical Bacteriophage Proteins Targeting Key Protein Complexes of

- Pseudomonas aeruginosa*. Journal of Proteome Research 13: 4446–4456. doi: [10.1021/pr500796n](https://doi.org/10.1021/pr500796n) PMID: [25185497](https://pubmed.ncbi.nlm.nih.gov/25185497/)
54. Wagemans J, Blasdel BG, Van den Bossche A, Uytterhoeven B, De Smet J, et al. (2014) Functional elucidation of antibacterial phage ORFans targeting *Pseudomonas aeruginosa*. Cellular Microbiology 16: 1822–1835. doi: [10.1111/cmi.12330](https://doi.org/10.1111/cmi.12330) PMID: [25059764](https://pubmed.ncbi.nlm.nih.gov/25059764/)
  55. Wagemans J, Delattre A-S, Uytterhoeven B, De Smet J, Cenens W, Aertsen A, et al. (2015) Antibacterial phage ORFans of *Pseudomonas aeruginosa* phage LUZ24 reveal a novel MvaT inhibiting protein. Frontiers in Microbiology 6.
  56. Van den Bossche A, Hardwick SW, Ceyskens P-J, Hendrix H, Voet M, Dendooven T, et al. (2016) Structural elucidation of a novel mechanism for the bacteriophage-based inhibition of the RNA degradesome. eLife 5: e16413. doi: [10.7554/eLife.16413](https://doi.org/10.7554/eLife.16413) PMID: [27447594](https://pubmed.ncbi.nlm.nih.gov/27447594/)
  57. Kropinski A, Mazzocco A, Waddell T, Lingohr E, Johnson R (2009) Enumeration of Bacteriophages by Double Agar Overlay Plaque Assay. In: Clokie MJ, Kropinski A, editors. Bacteriophages: Humana Press. pp. 69–76.
  58. Sambrook J (2001) Molecular cloning: a laboratory manual; Russell DW, editor. Cold Spring Harbor, New York: Cold Spring Harbor Laboratory.
  59. Ackermann H-W (2009) Basic Phage Electron Microscopy. In: Clokie MJ, Kropinski A, editors. Bacteriophages: Humana Press. pp. 113–126.
  60. Kutter E (2009) Phage host range and efficiency of plating. In: Clokie MJ, Kropinski A, editors. Bacteriophages: Humana Press. pp. 141–149.
  61. Schneider CA, Rasband WS, Eliceiri KW (2012) NIH Image to ImageJ: 25 years of image analysis. Nat Meth 9: 671–675.
  62. Wessel D, Flügge UI (1984) A method for the quantitative recovery of protein in dilute solution in the presence of detergents and lipids. Analytical Biochemistry 138: 141–143. PMID: [6731838](https://pubmed.ncbi.nlm.nih.gov/6731838/)
  63. Field D, Tiwari B, Booth T, Houten S, Swan D, Bertrand N, et al. (2006) Open software for biologists: from famine to feast. Nature Biotechnology 24: 801–803. doi: [10.1038/nbt0706-801](https://doi.org/10.1038/nbt0706-801) PMID: [16841067](https://pubmed.ncbi.nlm.nih.gov/16841067/)
  64. Besemer J, Borodovsky M (1999) Heuristic approach to deriving models for gene finding. Nucleic Acids Research 27: 3911–3920. PMID: [10481031](https://pubmed.ncbi.nlm.nih.gov/10481031/)
  65. Delcher AL, Harmon D, Kasif S, White O, Salzberg SL (1999) Improved microbial gene identification with GLIMMER. Nucleic Acids Research 27: 4636–4641. PMID: [10556321](https://pubmed.ncbi.nlm.nih.gov/10556321/)
  66. Hyatt D, Chen G-L, LoCascio P, Land M, Larimer F, Hauser L (2010) Prodigal: prokaryotic gene recognition and translation initiation site identification. BMC Bioinformatics 11: 119. doi: [10.1186/1471-2105-11-119](https://doi.org/10.1186/1471-2105-11-119) PMID: [20211023](https://pubmed.ncbi.nlm.nih.gov/20211023/)
  67. Rutherford K, Parkhill J, Crook J, Horsnell T, Rice P, Rajandream MA, et al. (2000) Artemis: sequence visualization and annotation. Bioinformatics 16: 944–945. PMID: [11120685](https://pubmed.ncbi.nlm.nih.gov/11120685/)
  68. Altschul SF, Gish W, Miller W, Myers EW, Lipman DJ (1990) Basic local alignment search tool. Journal of Molecular Biology 215: 403–410. doi: [10.1016/S0022-2836\(05\)80360-2](https://doi.org/10.1016/S0022-2836(05)80360-2) PMID: [2231712](https://pubmed.ncbi.nlm.nih.gov/2231712/)
  69. Altschul SF, Madden TL, Schäffer AA, Zhang J, Zhang Z, Miller W, et al. (1997) Gapped BLAST and PSI-BLAST: a new generation of protein database search programs. Nucleic Acids Research 25: 3389–3402. PMID: [9254694](https://pubmed.ncbi.nlm.nih.gov/9254694/)
  70. Marchler-Bauer A, Lu S, Anderson JB, Chitsaz F, Derbyshire MK, DeWeese-Scott C, et al. (2011) CDD: a Conserved Domain Database for the functional annotation of proteins. Nucleic Acids Research 39: D225–D229. doi: [10.1093/nar/gkq1189](https://doi.org/10.1093/nar/gkq1189) PMID: [21109532](https://pubmed.ncbi.nlm.nih.gov/21109532/)
  71. Punta M, Coghill PC, Eberhardt RY, Mistry J, Tate J, Boursnell C, et al. (2012) The Pfam protein families database. Nucleic Acids Research 40: D290–D301. doi: [10.1093/nar/gkr1065](https://doi.org/10.1093/nar/gkr1065) PMID: [22127870](https://pubmed.ncbi.nlm.nih.gov/22127870/)
  72. Quevillon E, Silventoinen V, Pillai S, Harte N, Mulder N, Apweiler R, et al. (2005) InterProScan: protein domains identifier. Nucleic Acids Research 33: W116–W120. doi: [10.1093/nar/gki442](https://doi.org/10.1093/nar/gki442) PMID: [15980438](https://pubmed.ncbi.nlm.nih.gov/15980438/)
  73. Söding J (2005) Protein homology detection by HMM–HMM comparison. Bioinformatics 21: 951–960. doi: [10.1093/bioinformatics/bti125](https://doi.org/10.1093/bioinformatics/bti125) PMID: [15531603](https://pubmed.ncbi.nlm.nih.gov/15531603/)
  74. Söding J, Biegert A, Lupas AN (2005) The HHpred interactive server for protein homology detection and structure prediction. Nucleic Acids Research 33: W244–W248. doi: [10.1093/nar/gki408](https://doi.org/10.1093/nar/gki408) PMID: [15980461](https://pubmed.ncbi.nlm.nih.gov/15980461/)
  75. Bjellqvist B, Hughes G, Pasquali C, Paquet N, Ravier F, Sanchez JC, et al. (1993) The focusing positions of polypeptides in immobilized pH gradients can be predicted from their amino acid sequences. Electrophoresis 14: 1023–1031. PMID: [8125050](https://pubmed.ncbi.nlm.nih.gov/8125050/)

76. Krogh A, Larsson B, von Heijne G, Sonnhammer ELL (2001) Predicting transmembrane protein topology with a hidden markov model: application to complete genomes. *Journal of Molecular Biology* 305: 567–580. doi: [10.1006/jmbi.2000.4315](https://doi.org/10.1006/jmbi.2000.4315) PMID: [11152613](https://pubmed.ncbi.nlm.nih.gov/11152613/)
77. Petersen TN, Brunak S, von Heijne G, Nielsen H (2011) SignalP 4.0: discriminating signal peptides from transmembrane regions. *Nature Methods* 8: 785–786. doi: [10.1038/nmeth.1701](https://doi.org/10.1038/nmeth.1701) PMID: [21959131](https://pubmed.ncbi.nlm.nih.gov/21959131/)
78. Schattner P, Brooks AN, Lowe TM (2005) The tRNAscan-SE, snoscan and snoGPS web servers for the detection of tRNAs and snoRNAs. *Nucleic Acids Research* 33: W686–W689. doi: [10.1093/nar/gki366](https://doi.org/10.1093/nar/gki366) PMID: [15980563](https://pubmed.ncbi.nlm.nih.gov/15980563/)
79. Laslett D, Canback B (2004) ARAGORN, a program to detect tRNA genes and tmRNA genes in nucleotide sequences. *Nucleic Acids Research* 32: 11–16. doi: [10.1093/nar/gkh152](https://doi.org/10.1093/nar/gkh152) PMID: [14704338](https://pubmed.ncbi.nlm.nih.gov/14704338/)
80. Bailey TL, Boden M, Buske FA, Frith M, Grant CE, Clementi L, et al. (2009) MEME Suite: tools for motif discovery and searching. *Nucleic Acids Research* 37: W202–W208. doi: [10.1093/nar/gkp335](https://doi.org/10.1093/nar/gkp335) PMID: [19458158](https://pubmed.ncbi.nlm.nih.gov/19458158/)
81. Kingsford C, Ayanbule K, Salzberg S (2007) Rapid, accurate, computational discovery of Rho-independent transcription terminators illuminates their relationship to DNA uptake. *Genome Biology* 8: R22. doi: [10.1186/gb-2007-8-2-r22](https://doi.org/10.1186/gb-2007-8-2-r22) PMID: [17313685](https://pubmed.ncbi.nlm.nih.gov/17313685/)
82. Gruber AR, Lorenz R, Bernhart SH, Neuböck R, Hofacker IL (2008) The Vienna RNA Websuite. *Nucleic Acids Research* 36: W70–W74. doi: [10.1093/nar/gkn188](https://doi.org/10.1093/nar/gkn188) PMID: [18424795](https://pubmed.ncbi.nlm.nih.gov/18424795/)